available at www.sciencedirect.com

ScienceDirect

journal homepage: www.elsevier.com/locate/biochempharm

# Contribution of reactivated RUNX3 to inhibition of gastric cancer cell growth following suberoylanilide hydroxamic acid (vorinostat) treatment

*Canhua Huang* [a], *Hiroshi Ida* [b], *Kosei Ito* [a,b], *Haiyuan Zhang* [a], *Yoshiaki Ito* [a,b,*]

[a] *Oncology Research Institute, National University of Singapore, Singapore*
[b] *Institute of Molecular and Cell Biology, Proteos, 61 Biopolis Drive, Singapore 138673, Singapore*

ARTICLE INFO

*Article history:*
Received 23 October 2006
Accepted 11 December 2006

*Keywords:*
Vorinostat
*RUNX3*
Gastric cancer
Chemotherapy

ABSTRACT

Vorinostat (suberoylanilide hydroxamic acid, SAHA) represents a new class of highly potent histone deacetylase (HDAC) inhibitors that cause growth arrest, differentiation, and apoptosis of many tumor types *in vitro* and *in vivo*. *RUNX3*, a gastric tumor suppressor, is epigenetically silenced in gastric cancer cells. This study investigates the role of *RUNX3* in vorinostat-induced suppression of gastric cancer cell growth. *RUNX3* was up-regulated by vorinostat in gastric cancer cell lines not expressing *RUNX3*. In terms of cell viability, the mean $IC_{50}$ of vorinostat in *RUNX3*-negative cells was significantly lower than that seen in *RUNX3*-positive cells, indicating that the former are more sensitive to vorinostat in terms of growth arrest than are *RUNX3*-positive lines. The mechanism underlying this difference was found to be reactivation of *RUNX3* expression by vorinostat and concomitant increase in acetylated histone H3 in the promoter region of *RUNX3*. Using three *RUNX3*-negative cell lines, we determined the contribution of *RUNX3* reactivation to growth inhibition and induction of apoptosis following treatment of cells with vorinostat and found that up-regulated *RUNX3* was significantly responsible for tumor suppressive activities.



## 1. Introduction

Cancer is caused by accumulation of genetic and epigenetic changes in the somatic genome, resulting in aberrant expression of altered gene products or down-regulation of regulatory gene products [1]. Epigenetic events, recently recognized as critical in the development of cancer, are heritable alterations in gene expression occurring without changes in the DNA sequence. Such changes occur throughout in all stages of tumorigenesis, including the early phases, and are increasingly recognized as major mechanisms involved in silencing tumor suppressor genes [2]. Growing evidence suggests that aberrant chromatin remodeling represents the major mechanism of transcriptional gene silencing. Chromatin remodeling is controlled by opposing activities of histone acetylation and deacetylation [3,4]. Deacetylation of histones leads to compact nucleosomes and condensed chromatin, which is inaccessible to the transcriptional machinery and other DNA-binding proteins. Many tumor suppressor genes, such as $p15^{ink4b}$, $p16^{ink4a}$, $p21^{waf1}$, *TP53* and Rb, exhibit a cluster of CpG dinucleotides called CpG islands around promoter regions. In many cancer cells, CpG islands near tumor suppressor genes are highly methylated and recruit histone deacetylases to silence gene expression. Transcription is

* *Corresponding author at*: Institute of Molecular and Cell Biology, Proteos, 61 Biopolis Drive, Singapore 138673, Singapore.
E-mail address: Itoy@imcb.a-star.edu.sg (Y. Ito).

*Abbreviations:* SAHA, suberoylanilide hydroxamic acid; HDAC, histone deacetylase; HAT, histone acetylase; TSA, trichostatin A; ChIP, chromatin immunoprecipitation; MBD, methyl-CpG binding domain; DNMT, DNA methyltransferase; 5-aza-CdR, 5-aza-2′-deoxycytidine

0006-2952/$ – see front matter 
doi:10.1016/j.bcp.2006.12.013

initiated by local inhibition of HDAC and concomitant activation of histone acetylation in a chromatin segment. When the balance is shifted towards acetylation, the nucleosome structure opens, followed by unfolding of DNA, which facilitates transcription by enabling access to transcription factors.

Epigenetic changes can be reversed by small molecules, which are promising reagents for cancer chemotherapy. HDAC inhibitors (HDACIs) are a novel class of chemotherapeutic agents initially identified by the ability to reverse malignant phenotypes of transformed cells. They have been shown to activate differentiation programs, inhibit the cell cycle, and induce apoptosis in numerous tumor-derived cell lines [4]. Several classes of HDAC inhibitors have been identified, including (1) short chain fatty acids, e.g., butyrates, (2) hydroxamic acids, e.g., trichostatin A (TSA) and vorinostat, (3) cyclic tetrapeptides, and (4) benzamides [5–7]. Among them, vorinostat represents a new class of highly potent HDAC inhibitors that promote growth arrest, differentiation, and/or apoptosis in many tumor types in *vitro* and *in vivo*. Vorinostat is currently in Phase I & Phase II clinical trails, and encouraging results have been reported in treating hematological malignancies and solid tumors [3,8,9].

Three Runt-related (RUNX) genes, *RUNX1*, *RUNX2* and *RUNX3*, encode the DNA binding subunit of a heteromeric transcription factor, polyomavirus enhancer binding protein 2 (PEBP2)/core binding factor (CBF). These genes together with a related gene, *CBFB/Pebpb2*, which encodes the non-DNA binding subunit, are both developmental regulators and are important in human cancers or experimentally-induced mouse tumors [10]. *RUNX1* and *RUNX2* regulate haematopoiesis and osteogenesis, respectively [11]. *RUNX3* was identified as a strong gastric tumor suppressor candidate involved in 40–60% of gastric malignancies. Loss of *RUNX3* activity is due mainly to hemizygous deletions and epigenetic gene silencing [12]. More recently, mistargeting of RUNX3 to the cytoplasm has been recognized as an alternative mechanism in target gene inactivation. Inactivation of RUNX3 by hemizygous deletion and silencing combined with inactivation by mislocalization of the protein suggest that RUNX3 is inactivated in more than 80% of gastric cancer cases [13].

One mutation in RUNX3, RUNX3 (R122C), was found in a gastric cancer patient [12]; this mutation results in a protein defective in activating $p21^{WAF1/Cip1}$ which is defective in activating $p21^{WAF1/Cip1}$ in cooperation with TGF-β-activated SMAD [14]. Mutations in *RUNX3* are rare; nonetheless it is critical to determine the role of RUNX3 in cancer genesis, since epigenetic changes affect multiple genes, and it is difficult to assess whether RUNX3 is the one that contributes to tumorigenesis. More recently, loss-of-function mutations in *RUNX3* were observed in two cases of bladder cancer, although epigenetic silencing of *RUNX3* also occurs in these cancers. Significant inactivation of RUNX3 by cytoplasmic sequestration and DNA methylation has also been reported in breast cancer [16]. Finally, *RUNX3* is reportedly inactivated by methylation in many other cancers, including colorectal, lung, prostate, and liver cancers [17–20].

Our previous work demonstrated that a histone deacetylase inhibitor, trichostatin A, either alone or in combination with a DNA methyltransferase inhibitor, 5′-aza-2′-deoxycytidine, reactivated *RUNX3* in gastric cancer-derived cell lines that do not express *RUNX3*. Exogenous RUNX3 in a gastric cancer-derived cell line strongly inhibited tumor growth in nude mice, while exogenous RUNX3 (R122C) lacked such activity [10,12]. These observations suggest that HDAC inhibitors are attractive candidates for use in controlling gastric cancer cell growth [12].

In this study, we examine the ability of vorinostat to reactivate *RUNX3* expression in gastric cancer-derived cell lines and evaluate the role of RUNX3 as a tumor suppressor.

## 2. Materials and methods

### 2.1. Cell culture

Human gastric cancer cell lines MKN28, MKN74, NUGC-3, AGS, Kato III, MKN1, MKN45, SNU5, and SNU16 were obtained from the American Type Culture Collection (Rockville, MD), cultured in RPMI 1640 (Gibco-BRL Grand Island, NY) supplemented with 10% FBS and antibiotics (100 U of penicillin/ml and l00 μg streptomycin/ml) (Invitrogen), and grown at 37 °C in a 5% $CO_2$ atmosphere. SNU16 is a gastric cancer cell line expressing RUNX3 at a relatively high level. We usually use the level of the expressed RUNX3 in this cell line as a standard of the amount of RUNX3 in RUNX3 expressing cells [12,13]. Vorinostat was kindly provided by Aton Pharma Inc., a subsidiary of Merck & Co. Inc.

### 2.2. Plasmids

pcDNA-Flag-RUNX3 (1–187), a dominant negative form of RUNX3, and pEF-Bos-Flag-RUNX3 antisense were generated in our laboratory [13].

### 2.3. Cell growth inhibition assays

Vorinostat was dissolved and diluted in DMSO (10 mM stock solution). Gastric cancer cells were seeded in triplicate in 24-well dishes at a density of $2 \times 10^4$ cells/well, allowed to attach overnight, and the medium was replaced with medium containing the appropriate concentration of vorinostat (0, 2.5, 5, or 7.5 μM). Cell number was determined by counting using a hemocytometer at various times after initiation of vorinostat treatment, and cell viability was assessed by trypan blue dye exclusion.

To examine the effect of vorinostat on proliferation, cell growth was monitored in a 96-well plate format using the Cell Proliferation MTT Assay (Roche Applied Sciences, Cat #1465007) based upon metabolic cleavage of a tetrazolium salt to a colored formazan product. Briefly, $1.0 \times 10^4$ cells/well were seeded in 96-well plates in serum-containing medium and treated with 1–10 μM vorinostat for 72 h. MTT was added to each well following the manufacture's instruction. After incubation for 4 h at 37 °C, a solubilization solution was added, and the color reaction was quantified using the Ultramark Microplate Imaging System (Bio-Rad) at 550 nm with a reference filter of 690 nm. Three independent MTT assays were performed to determine the standard deviation. $IC_{50}$s were defined based on the vorinostat concentration required

to reduce the estimated cell number by 50% relative to untreated controls.

### 2.4. Apoptosis assay

Vorinostat-induced apoptosis was measured by a colorimetric assay using a cell death ELISA$^{plus}$ kit (Roche Applied Science, Indianapolis, IN, Cat #1774425) to quantitate *in vitro* levels of cytoplasmic histone-associated DNA fragments, an indicator of apoptosis. After vorinostat treatment, cells were lysed to release cytoplasmic histone-associated DNA fragments, and absorbance (ABS) was read at 405 nm with a reference filter of 490 nm. ABS was positively correlated with increased apoptosis. The data are reported as a percentage of untreated controls.

### 2.5. Cell cycle analysis

Flow cytometry analyses were performed using a FACScan flow cytometry system (Becton Dickinson, San Jose, CA) as described [21]. Briefly, cells were washed with PBS, fixed in 50% ice-cold ethanol/PBS for 30 min on ice, washed again with PBS, and resuspended and incubated in PI solution (70 μM propidium iodide, 38 mM sodium citrate, 20 μg/ml RNase A) for 30 min at 37 °C. Data were subsequently analyzed using winMDIv2.8 software.

### 2.6. RNA isolation and Taqman quantitative PCR

Total RNA was extracted from cell lines using an RNeasy mini-Kit (Qiagen, Valencia, CA). cDNA synthesis was performed with 2 μg total RNA using an oligo $(dT)_{15}$ primer (Roche) and Transcriptor Reverse Transcriptase using the primer system (Roche Applied Sciences). Assays-on-demands™ for *RUNX3* is Hs00231709_ml and for GAPDH is Hs00242386_ml. PCR amplification was performed using a 7000 Sequence Detection System (Applied Biosystems) under the following conditions: stage 1, 95 °C for 10 min, followed by 45 cycles of stage 2 at 95 °C for 15 s and 60 °C for 1 min. Relative levels of each mRNA were normalized to levels of GAPDH mRNA using 7000 Real Time PCR System Sequence Detection Software (Applied Biosystems).

### 2.7. SDS-PAGE and Western blotting

MKN28 cells ($0.5 \times 10^7$ to $1.0 \times 10^7$) were cultured as described below without and with 1–7.5 μM vorinostat for 4–24 h. For histone preparation, cells were harvested and washed with PBS and resuspended in 1 ml ice-cold lysis buffer (10 mM Tris–HCl, pH 6.5, 50 mM sodium bisulfite, 1% Triton X-100, 10 mM $MgCl_2$, 8.6% sucrose) before homogenization with two dounce strokes. Nuclei were pelleted at 700 rpm in a Beckman GS-6R centrifuge for 5 min and washed 3 times with 1 ml of lysis buffer. The final wash was performed with 1 ml of Tris–EDTA solution (10 mM Tris–HCl, pH 7.4, 13 mM EDTA). Nuclei were then pelleted and resuspended in 100 μl of ice-cold water. Sulfuric acid was added to the samples to a final concentration of 0.2 M, and then samples were vortexed and incubated on ice for 1 h. Samples were centrifuged at 15,000 × *g* for 10 min at 4 °C, and the supernatant was precipitated with 1 ml of acetone overnight at −20 °C. Precipitated protein was collected by centrifugation at 15,000 × *g* for 10 min at 4 °C, air dried, and resuspended in 50–100 μl of water. Protein concentrations of lysates and histone preparations were determined using the Bio-Rad Protein Assay kit with BSA as the standard. Proteins (1–25 μg) were denatured at 100 °C in loading buffer for 10 min and electrophoresed on 12% polyacrylamide gels. After electrophoresis, samples were transferred onto nitrocellulose (0.45 μm) in buffer containing 0.25 M Tris-base (pH 8.3), 1.86 M glycine, and 20% methanol for 2 h at 4 °C. To verify equal protein loading, a parallel protein gel was run and stained with Coomassie blue G250. For Western blotting, PVDF membranes were incubated in PBS plus 3% milk for 30 min at room temperature. That buffer was replaced with PBS plus 3% milk containing the specific rabbit polyclonal antiserum diluted 1:1000 and then incubated at 4 °C for 16 h. Samples (nuclei treated or untreated with vorinostat) were kept on ice for 30 min before centrifugation at 15,000 × *g* for 10 min at 4 °C. The following antibodies were used: rabbit anti-human acetylated histone H3 and rabbit anti-human acetylated histone H4 (Upstate Biotechnology, Upstate, NY). PVDF membranes were washed in distilled water and then incubated in PBS containing 3% milk and a 1:5000 dilution of goat anti-rabbit horseradish peroxidase for 2 h at room temperature. Blots were washed in distilled water, rinsed, and subjected to the enhanced chemiluminescence detection reaction, according to the manufacturer's instructions (Amersham Pharmacia Biotechnology, Amersham, Bucks, UK).

### 2.8. Chromatin immunoprecipitation PCR: ChIP-PCR

Chromatin immunoprecipitation was performed using the acetyl-histone H3 and H4 immunoprecipitation (ChIP) Assay Kit (Upstate Biotechnology, Upstate, NY), following the manufacturer's instructions. Briefly, after culturing MKN28 cells with or without 2.5 μM vorinostat for 12 h, formaldehyde was added to crosslink histones to DNA. Cells were harvested and sonicated in SDS lysis buffer to shear DNA to approximately 200–500 bp. Lysates were then collected for immunoprecipitation. To reduce non-specific background, a 50% slurry of salmon sperm DNA/protein A agarose was added to the lysate. After brief centrifugation, immunoprecipitation of supernatant proteins was performed with antibodies to human acetyl H3 at 4 °C with agitation. Subsequently, the slurry was added to form a protein A agarose/antibody/histone complex, and the histone complex was eluted in elution buffer (1% SDS, 0.1 M $NaHCO_3$). Recovery of DNA from histones was achieved by proteinase K digestion, phenol/chloroform extraction, and ethanol precipitation. Pellets were dissolved in appropriate buffer and used for PCR using four pairs of primers targeting *RUNX3* sequences in the region from −2821 bp of the promoter region to +2267 downstream of the transcription start site. Those pairs were: A (−2821 to −2686): 5′-agg tgg aaa ttg gga aca agc tag cc-3′ (sense), 5′-ag aca aac cga tgg ctt tgt gtc aaa-3′ (antisense); B (−1187 to −1047): 5′-tgt ttt tca aag agc cac agg ccg cc-3′ (sense), 5′-ggg agt ctc cta ggg acc cta agt ag-3′ (antisense); C (+450 to +567): 5′-gtt ccg ttt tgg atg cgc cct gca-3′ (sense), 5′-ca aaa ccc cat ccg ccc att tcc gca-3′ (antisense); D (+2137 to +2267): 5′-ggt ggt ggc att ggg gga cgt gcc gga-3′ (sense), 5′-gtc gtt gaa cct ggc cac ctg gtt ctt-3′ (antisense). The resulting amplicons were approximately 110–140 bp long and were visualized on 2% agarose gels following ethidium bromide staining.

## 3. Results

### 3.1. Effects of vorinostat on gastric cancer-derived cell lines in vitro

RUNX3 expression in gastric cancer cells was examined in our previous studies [12,13]. In 40–50% of the gastric cancer cases, RUNX3 was silenced by hypermethylation of the promoter region and in additional 40% cases RUNX3 was inactivated by protein mislocalization. To examine vorinostat cytotoxicity, 11 human gastric cancer cell lines were cultured in the presence of increasing concentrations of vorinostat (0–10 μM) for 3 days, and proliferation of gastric cancer cells was measured using an MTT Assay. The $IC_{50}$ of the mean of the six RUNX3 negative cell lines was 3.10, whereas that in 5 RUNX3 expressing cells was 5.76. Four cell lines, MKN1, MKN45, SNU1 and SNU5, were particularly resistant to vorinostat, and MKN45 was highly insensitive to vorinostat ($IC_{50} > 8$ μM) (Fig. 1). RUNX3-negative gastric cancer cells were more sensitive to vorinostat treatment than were RUNX3-positive cells, with a few exceptions (Fig. 1), suggesting that RUNX3 may be reactivated by vorinostat treatment.

### 3.2. Reactivation of transcriptionally silenced RUNX3 by vorinostat

Three gastric cancer cell lines—MKN28, MKN74, NUGC-3—which do not express *RUNX3* due to hypermethylation of CpG islands in the promoter region, were selected for vorinostat treatment. Vorinostat at 2.5–7.5 μM effectively reactivated *RUNX3* expression in these lines within 24 h, and quantitative RT-PCR showed that *RUNX3* transcripts peaked at around 48 h (Fig. 2). Levels of reactivated RUNX3 RNA were highest at 7.5 μM

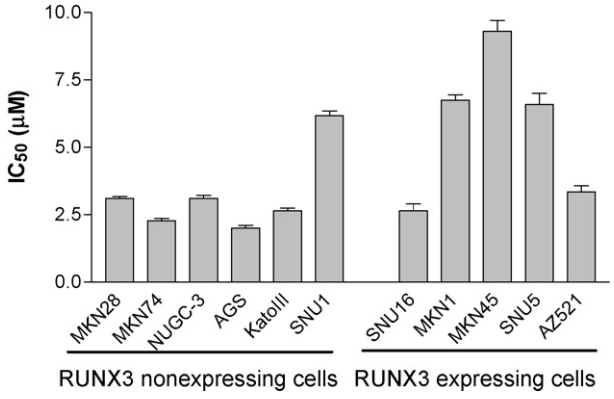


**Fig. 1 – Proliferation of and toxicity to gastric cancer cells following vorinostat treatment. The mean $IC_{50}$ of RUNX3 non-expressing gastric cancer cells (3.2 ± 1.54 μM, $n = 6$,) was lower than that of the RUNX3-expressing cells (5.9 ± 2.77 μM, $n = 5$), a statistically significant difference ($p < 0.05$). $IC_{50}$ was defined as the vorinostat concentration at which a 50% reduction in cell viability was seen compared to untreated controls after 3 days of treatment. Cell growth was monitored in a 96-well plate format using the Cell Proliferation MTT Assay. Bars represent standard deviations (±S.D.) based on three independent experiments.**

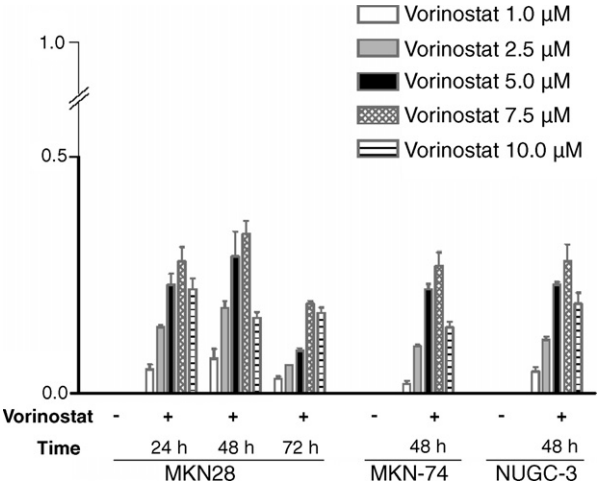


**Fig. 2 – Dose- and time-dependent reactivation of *RUNX3* following treatment with vorinostat. The MKN28 line was treated with 0 μM (DMSO)–10 μM vorinostat for 24–72 h, total RNA was isolated, and cDNA was synthesized as described in Section 2. *RUNX3* transcripts were measured by real time PCR. MKN28 cells or cells plus DMSO vehicle served as controls. SNU16, a *RUNX3*-expressing gastric cancer cell line, served as a positive control. Three independent experiments were carried out, and the mean value representing levels of RUNX3 transcripts from a typical experiment is indicated.**

vorinostat and the maximum level of mRNA was about 30% of that observed in SNU16, a line expressing RUNX3 [12]. This observation is consistent with our earlier studies showing that another histone deacetylase inhibitor, trichostatin A, effectively reactivates *RUNX3* expression in gastric cancer cells [12].

### 3.3. Accumulation of acetylated histones following vorinostat treatment

Since vorinostat inhibits histone deacetylase, cells treated with vorinostat are predicted to show elevated levels of acetylated histones. Western blotting of MKN28 cell nuclear lysates with antibodies to acetylated histones H3 and H4 showed that vorinostat increased acetylation of histones in both a time- and dose-dependent manner (Fig. 3a and b). Time-course analysis showed significant accumulation of acetylated histones within 4 h, peaking at around 24 h. Treatment of MKN28 cells with various concentrations of vorinostat (0–7.5 μM) indicated incremental accumulation of acetylated histone H3 and H4. No further increase was observed at concentrations greater than 5 μM.

### 3.4. Accumulation of acetylated histones in chromatin associated with RUNX3 following vorinostat treatment

Chromatin immunoprecipitation PCR (ChIP-PCR) was performed to determine whether reactivation of *RUNX3* was associated with the inhibition of HDAC activity in gastric cancer cells. Four pairs of primers complementary to *RUNX3*—from the upstream promoter region to downstream of the

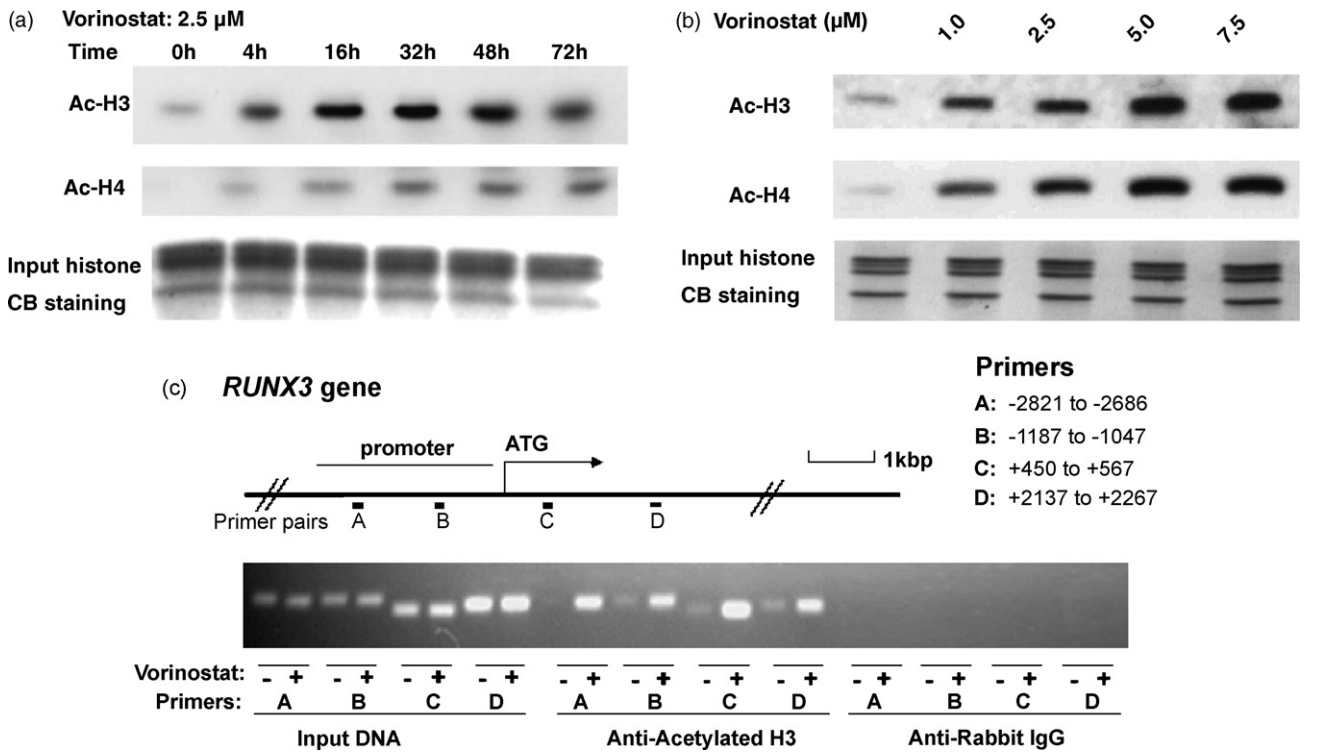


**Fig. 3 – (a and b) Vorinostat stimulates histone acetylation in a dose- and time-dependent manner. MKN28 cells were treated with 2.5 μM vorinostat for the indicated times (a) or treated with the indicated concentrations of vorinostat for 12 h (b). Cells were harvested, and histones were prepared as described in Section 2. Histone acetylation was detected by Western blotting with antibodies against acetylated H3 and H4. The *top panel* shows acetylated histone H3, the *middle panel* contains acetylated histone H4, and the *bottom panel* shows a Coomassie blue-stained gel of total histones extracted from cells. (c) Vorinostat-induced accumulation of acetylated histone H3 or H4 in chromatin associated with *RUNX3*. The *top panel* is a schematic representation of *RUNX3* indicating the location of four primer pairs used for PCR amplification in ChIP assays. Chromatin fragments from cells cultured with and without vorinostat (5 μM) for 12 h were immunoprecipitated with an antibody to acetylated histone H3 in MKN28 cells. The *bottom panel* shows ChIP assays prepared using anti-diacetylated H3 or rabbit normal IgG.**

transcriptional start site—were used (see Section 2). ChIP-PCR analysis indicated a remarkable increase in levels of PCR products from vorinostat-treated cells, compared with the same region from untreated cells (Fig. 3c), suggesting that *RUNX3* is one of the reactivated genes in response to vorinostat induction.

### 3.5. *Inhibition of proliferation of gastric cancer-derived cells by vorinostat*

Since RUNX3 expression is associated with inhibition of cell growth, we examined the effect of vorinostat on cell proliferation. After addition of vorinostat to cell cultures, the number of live cells was determined by a trypan blue exclusion assay. No difference was observed between cells stably transfected with vector only and parental cells which had never been transfected with any vectors following treatment with vorinostat (data not shown). We observed that vorinostat induced a significant cell growth inhibition (Fig. 4). Because vorinostat could re-activate several genes in addition to *RUNX3*, we examined the extent of the contribution of re-activated *RUNX3* to growth inhibition by comparing proliferation of MKN28 and MKN74, two lines stably transfected with pcDNA-Flag-RUNX3 (1–187), which encodes a dominant negative form of RUNX protein, in the presence of vorinostat. Vorinostat significantly inhibited growth of MKN28 and MKN74 lines, but expression of the dominant negative form of RUNX3 reduced its growth inhibitory activity (Fig. 4a and b). These results suggest that re-activated *RUNX3* significantly contributes to growth inhibitory effects induced by vorinostat.

Proliferation was also compared between NUGC-3 cells with or without stably transfected *RUNX3* antisense cDNA following treatment with vorinostat. This antisense construct is specific for RUNX3 and does not interfere with RUNX1 or RUNX2 activity. Treatment with *RUNX3* antisense also significantly reduced the growth inhibitory effect of vorinostat (Fig. 4c).

### 3.6. *RUNX3 contributes to induction of apoptosis following vorinostat treatment*

HDACs reactivate many genes, particularly tumor suppressors, that are silenced by hypermethylation of promoter regions [22,23]. Vorinostat has been shown to inhibit cell growth and induce apoptosis in several cancer cell lines [4].

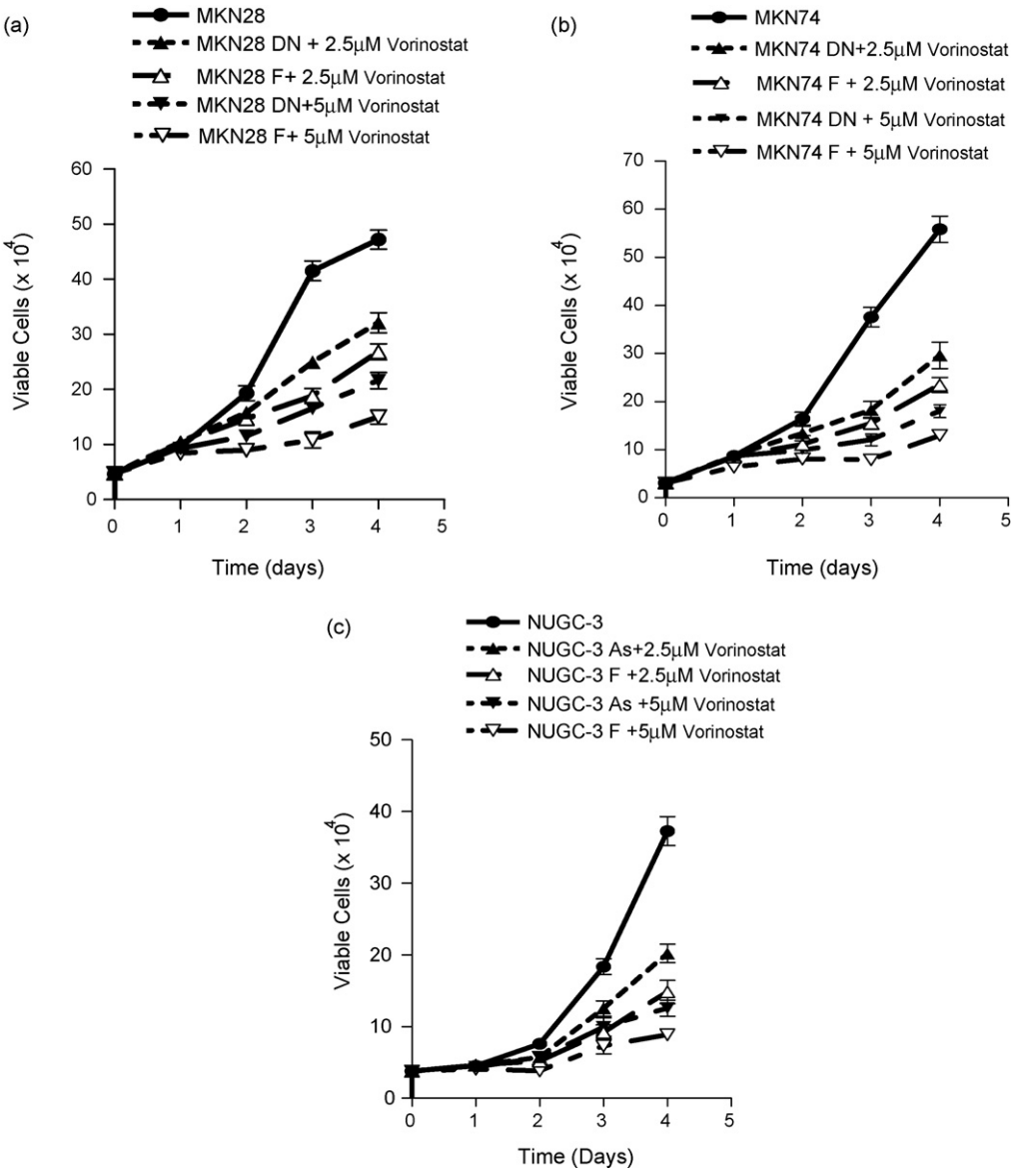


**Fig. 4 – Effects of vorinostat on gastric cancer cells *in vitro*. Cells (MKN28, MKN74, or NUGC-3) were treated with vorinostat at the following concentrations: 0 (control) (●); 2.5 μM vorinostat (▲); 5 μM vorinostat (▼). Cells transfected with a pcDNA-*RUNX3* dominant negative plasmid (MKN28 DN and MKN74 DN) or pEF-Bos-*RUNX3* antisense cDNA (NUGC-3 AS). In the control experiments, cells were transfected with either pcDNA-Flag or pEF-Bos-Flag (MKN28 F, MKN74 F, and NUGC-3 F). Cells were treated with vorinostat at the following concentrations: 2.5 μM (△); 5 μM (▽). Cells were counted at indicated times using a hemocytometer, and the number of viable cells was determined by trypan blue exclusion. Data are presented as means ± S.E. of triplicate values from a typical experiment.**

Although induction of apoptosis or cell cycle arrest by vorinostat could be due to effects of more than one reactivated gene, we evaluated the contribution of *RUNX3* to vorinostat-induced apoptosis. Apoptosis observed in MKN28 and MKN74 cells stably expressing a dominant negative form of RUNX in the presence of various concentrations of vorinostat is shown in Fig. 5. Vorinostat induced apoptosis in those cells in dose-dependent manner (Fig. 5a and b, dotted line). Interestingly, at 3–5 μM vorinostat, induction of apoptosis was significantly reduced in the presence of the dominant negative form of *RUNX3* (Fig. 5a and b, solid line), strongly suggesting that reactivated RUNX protein(s) significantly contribute to induction of apoptosis. Consistent with this result, induction of apoptosis by vorinostat was also significantly suppressed in the NUGC-3 line stably transfected with *RUNX3* antisense cDNA (Fig. 5c). These results establish that *RUNX3* contributes significantly to induction of apoptosis following re-activation by vorinostat.

### 3.7. *Cell cycle analysis of vorinostat-treated gastric cancer cell lines*

Because HDACIs can affect both cell proliferation and cell survival, we assessed the effect of vorinostat treatment on the

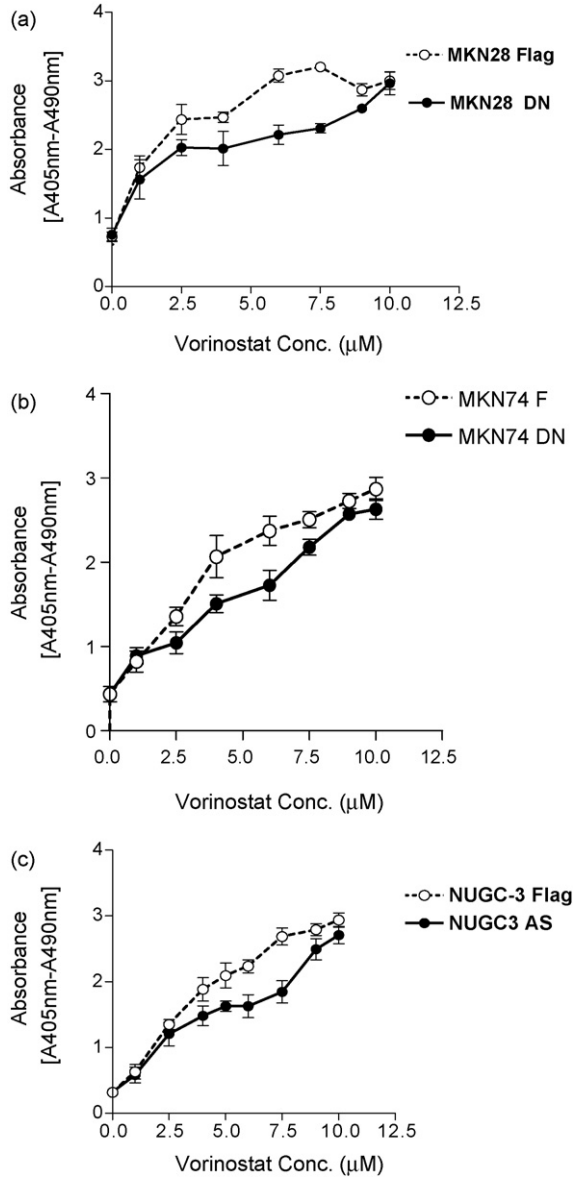


**Fig. 5 – Assessment of apoptosis in response to vorinostat treatment. MKN28, MKN74, and NUGC-3 lines transfected with pcDNA-Flag RUNX3 dominant negative, pEFBOS-Flag *RUNX3* antisense cDNA (○), or pcDNA-Flag or pEFBos-Flag vectors (●) were treated with (0–10 μM vorinostat) for 24 h. Apoptosis was measured using a cell death ELISA$^{plus}$ kit (Roche Applied Science), following the manufacturer's instructions. The *x*-axis indicates vorinostat concentration, and absorbance (ABS) on the *y*-axis represents the relative apoptosis as a percentage of untreated controls. Bars represent standard deviations of three independent experiments.**

cell cycle and asked if *RUNX3* played a role in this process. MKN28, MKN74, and NUGC-3 and these lines stably transfected with pcDNA-Flag-*RUNX3* (dominant negative) or pEF-BOS-Flag-*RUNX3* (anti-sense cDNA) were cultured with 0–7.5 μM vorinostat for 0–72 h and subjected to flow cytometric analysis. Cells transfected with mock plasmids pcDNA-Flag or pEF-BOS-Flag displayed the same cell cycle distribution pattern as parental cells (data not shown). Time-course analysis showed that treatment with 5 μM vorinostat induced G2/M arrest at 24 h in all lines. However, the percentage of G2/M cells in MKN28 and NUGC-3 decreased rapidly at 48 h, concomitant with a rapid increase in the percentage of apoptotic cells (Sub-G1), and movement of cells through G2/M phase may precede apoptosis (Fig. 6a and c). In contrast to MKN28 and NUGC-3 cells, MKN74 cells remained in G2/M arrest in a dose-dependent manner until 72 h, as indicated (Fig. 6b). Our observations are consistent with the idea that vorinostat's effect on cell cycle progression is cell type specific [24].

Restoration of *RUNX3* expression by vorinostat treatment was abolished in cells transfected with either dominant negative *RUNX3* or *RUNX3* antisense cDNA. FACS analysis revealed that the percentage of apoptotic cells was markedly reduced in these cells compared with mock controls. On the other hand, loss of *RUNX3* expression appeared to increase the percentage of cells in G0/G1 and G2/M in lines MKN28 and MKN74 in dose- and time-dependent manner (Fig. 6a and b), whereas the only remarkable increase in the G0/G1 percentage was observed in line NUGC-3 (Fig. 6c). Our observations suggest that *RUNX3* plays a role in vorinostat-mediated cell cycle changes, and the presence of RUNX3 likely promotes apoptosis of arrested cells. As demonstrated in Fig. 6a–c, vorinostat induced dose-dependent apoptosis of gastric cancer cells. However, a remarkable reduction in the number of apoptotic cells was observed if *RUNX3* re-expression was inhibited. These observations are consistent with data obtained in separate apoptotic assays (Fig. 6a–c) and indicate that *RUNX3* contributes significantly to gastric cancer cell apoptosis in response to vorinostat.

## 4. Discussion

In this study, we evaluated the potential contribution of RUNX3 to cell growth inhibition and apoptosis when cell lines lacking RUNX3 expression were treated with vorinostat. Vorinostat induced accumulation of acetylated histones in *RUNX3* chromatin, an increase associated with up-regulation of *RUNX3* in three cell lines examined. As expected, vorinostat induced cell cycle arrest and apoptosis. Inhibition of RUNX3 function by either a dominant negative form of RUNX protein or antisense *RUNX3* significantly reduced growth and apoptosis inhibitory activities of vorinostat, suggesting that of all genes potentially reactivated by vorinostat, *RUNX3* contributes significantly to the process. These findings indicate that growth inhibition of human gastric cancer cells by vorinostat may be due in part to rescue of expression of the major gastric tumor suppressor *RUNX3*.

How the dominant negative form of RUNX3 (1–187) interferes with RUNX3 function and possibly that of RUNX1 and RUNX is not clear. RUNX3 (1–187) contains the DNA binding domain but lacks the trans-activation domain and other important functions associated with the C-terminus. Since such truncated proteins bind DNA more readily than the full-length protein, RUNX3 (1–187) could compete with full-length RUNX proteins for DNA binding [25]. Recently, we

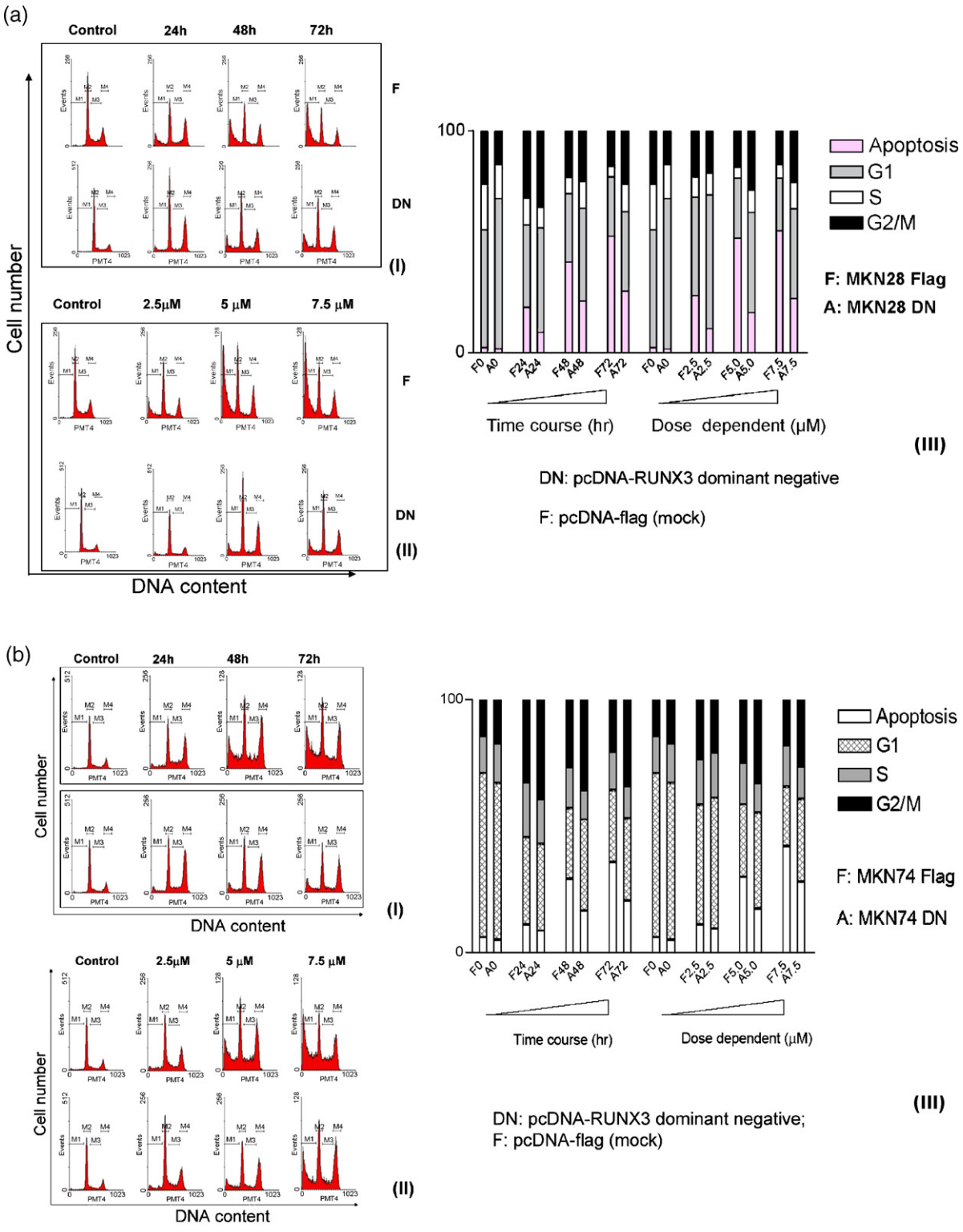


**Fig. 6 – Vorinostat induces cell cycle arrest and apoptosis in gastric cancer cells. MKN28, MKN74, and NUGC-3 cells were treated with 5 μM vorinostat for 0–72 h, or with the indicated concentration of vorinostat for 72 h. Cells were harvested, stained with propidium iodide (PI), and analyzed for cell cycle distribution by flow cytometry. Shown are time-dependent DNA histograms and dose-dependent DNA histograms (II). MKN28, MKN74, and NUGC-3 cells transfected with pcDNA-*RUNX3* dominant negative or pEFBos-RUNX3 antisense cDNA are shown in the *top panel*, while cells transfected with pcDNA-Flag or pEFBos-Flag control are shown in the *bottom panel*. M1–M4 represent sub G1 (apoptotic cells), G1, S, G2/M phases, respectively. The proportion of cells at different stages of the cell cycle and the percentage of apoptotic cells are shown in a–c (III).**

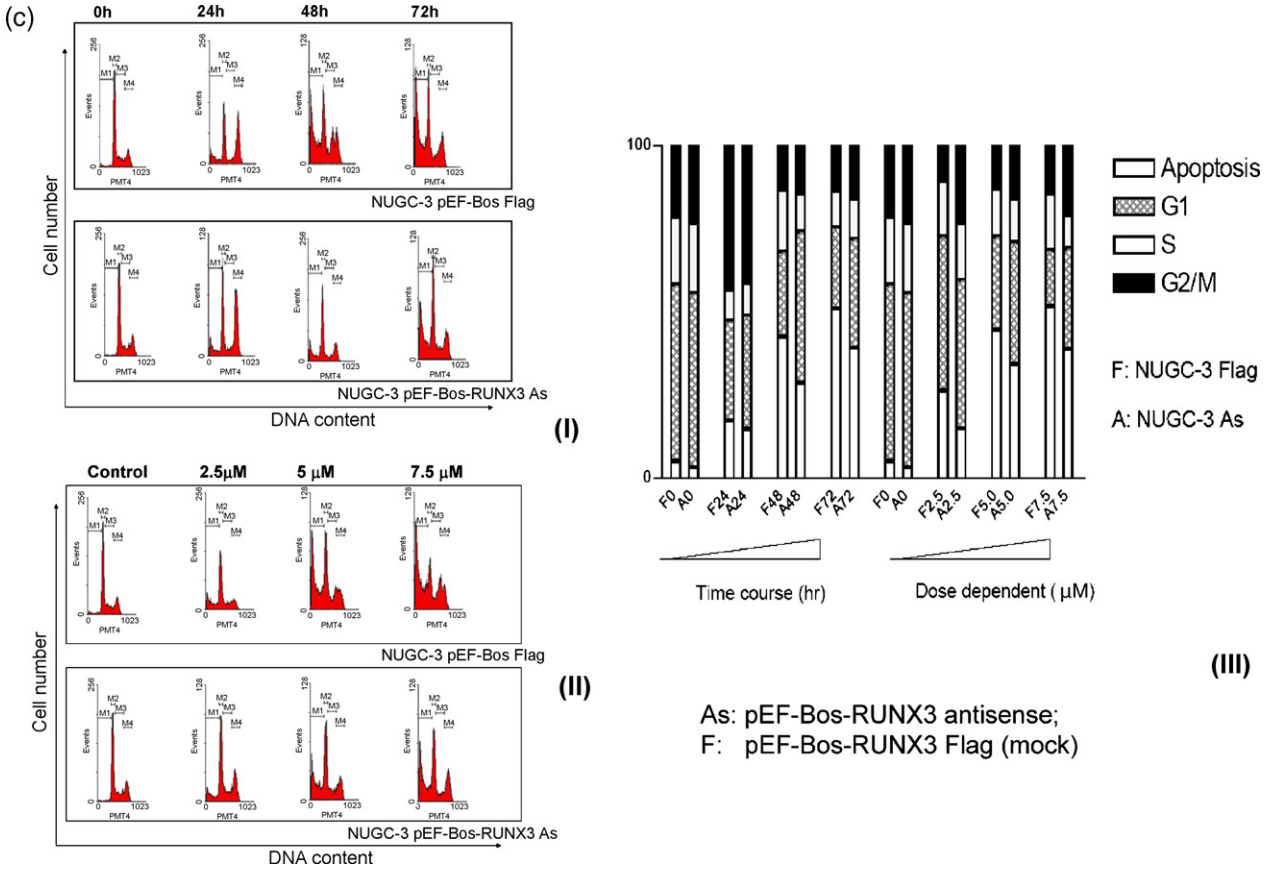


**Fig. 6. (Continued).**

observed that exogenous RUNX3 (1–187) is localized in the cytoplasm of some gastric cancer-derived cells. Thus such a truncation of exogenous RUNX3 could anchor endogenous RUNX3 to the cytoplasm by an unknown mechanism, thereby inactivating it [13]. In any event, complete inactivation of RUNX3 is not expected by either of the two mechanisms. Inactivation of *RUNX3* by antisense DNA also is likely partial. Thus our observation that these loss-of-function molecules reverse the inhibitory effect of vorinostat up to about 30% is quite significant. These results emphasize the importance of *RUNX3* among tumor suppressor genes presumed to be reactivated by vorinostat. Reactivation of *RUNX3* in gastric cancer cells, therefore, may have significant therapeutic effect. It is worth emphasizing that *RUNX3* is inactivated by epigenetic silencing in 40–60% of gastric cancer cases. Reactivated *RUNX3* inhibits cell growth and promotes apoptosis. In most cases, reactivated *RUNX3* lacks mutation [12]. In fact, *RUNX3* is frequently inactivated in many types of cancer, including the major ones, by promoter methylation. Some evidence suggests that *RUNX3* inactivation occurs at very early stages of gastric and breast cancers [12,16]. If so, these observations overall suggest that HDAC inhibitors are potentially useful for chemoprevention of several types of cancer.

DNA methylation and histone modification represent two epigenetic events [26]. A growing number of studies demonstrate synergy of HDAC inhibitors and DNMT inhibitors in reactivating tumor suppressor genes and their potential anticancer activities [27,28]. The DNMT inhibitor 5-aza-2′-deoxycytidine (5-aza-CdR) induces terminal differentiation or senescence of cancer cells in leukemia and lung cancer. A combination of 5-aza-CdR and HDAC inhibitors reportedly produced a synergistic reaction on tumor suppressor genes $p15^{CDKN2B}$ and $p16^{CDKN2A}$, as well as the cancer-related gene TIMP3 and the DNA repair gene MLH1 [29,30]. Consistent with these reports, our previous work demonstrated that combining 5-aza-CdR with the HDAC inhibitor TSA very efficiently induced *RUNX3* re-expression [12]. Based on this observation, future work will examine a potential cooperative effect of vorinostat and 5-aza-CdR on reactivation of silenced *RUNX3* in order to determine if such a strategy could increase efficacy against gastric cancer and reduce toxicity.

RUNX proteins are among numerous targets of the TGF-β superfamily [31]. TGF-β has been shown to cause cell cycle arrest by inhibiting Cdk activities and thereby inducing expression of the Cdk inhibitor $p21^{WAF1/CIP1}$ [32,33]. HDAC inhibitors cause cell cycle arrest at G0/G1 or G2 in several types of cancer cell through selective up-regulation of $p21^{WAF1/CIP1}$ [2,34–36]. Our data demonstrate that vorinostat induced G2/M arrest in the gastric cancer cell lines examined. Reactivation of *RUNX3* increased the number of cells arrested in G2/M in response to vorinostat (Fig. 6a–c). Indeed, we have shown that $p21^{WAF1/Cip1}$ is transcriptionally induced by RUNX3 in gastric epithelial cells in cooperation with Smads [14]. Therefore, vorinostat likely induces $p21^{WAF1/Cip1}$ by reactivating RUNX3.

It is widely accepted that chemotherapeutic drugs can induce cell death by activating one of two major apoptotic pathways: the death receptor pathway and the intrinsic mitochondrial pathway. Several groups have provided evidence that vorinostat mediates apoptosis in various cell lines via a novel mechanism involving activation of an intrinsic death pathway by promoting caspase-independent cleavage and activation of Bid [37,38]. Our data suggest that loss of *RUNX3* expression results in remarkably reduced apoptosis. We recently reported that RUNX3 induces apoptosis of gastric epithelial cells by activating expression of a Bcl-2 family protein, Bim, a proapoptosis gene, by two different mechanisms: by inducing Bim in collaboration with Smads in a TGF-β-dependent manner [39] and by activating Bim transcription in a TGF-β-independent manner through interaction of RUNX3 with the forkhead factor, FoxO3a [40]. RUNX3 may directly trigger the mitochondrial apoptotic program by up-regulating Bim in response to vorinostat.

Vorinostat reportedly inhibits tumor cell growth in various animal models [3,41], although the detailed mechanisms are not known. Our study demonstrates that vorinostat induces re-expression of a major gastric tumor suppressor *RUNX3*, and reactivation of *RUNX3* contributes significantly to inhibition of gastric cancer cell growth *in vitro*. Using an established *RUNX3* (−/−) cancer model, analogous *in vivo* studies are now possible.

## Acknowledgement

This work was financially supported by grant NMRC/0889/2004 from Singapore.

## REFERENCES

[1] Jaenisch R, Bird A. Epigenetic regulation of gene expression: how the genome integrates intrinsic and environmental signals. Nat Genet 2003;33:245–54.
[2] Kopelovich L, Crowell JA, Fay JR. The epigenome as a target for cancer chemoprevention. J Natl Cancer Inst 2003;95(23):1747–57.
[3] Marks PA, Rifkind RA, Richon VM, Breslow R, Miller T, Kelly WK. Histone deacetylases and cancer: causes and therapies. Nat Rev Cancer 2001;1(3):194–202.
[4] Johnstone RW, Ruefli AA, Lowe SW. Apoptosis: a link between cancer genetics and chemotherapy. Cell 2002;108:153–64.
[5] Yoshida M, Shimazu T, Matsuyama A. Protein deacetylases: enzymes with functional diversity as novel therapeutic targets. Prog Cell Cycle Res 2003;5:269–78.
[6] Curtin M, Glaser K. Histone deacetylase inhibitors: the Abbott experience. Curr Med Chem 2003;10(22):2373–92.
[7] Delorme BA. Novel hydroxamate and anilide derivatives as potent histone deacetylase inhibitors: synthesis and antiproliferative evaluation. Curr Med Chem 2003;10(22):2359–72.
[8] Marks PA, Richon VM, Miller T, Kelly WK. Histone deacetylase inhibitors. Adv Cancer Res 2004;91:137–68.
[9] Remiszewski S. The discovery of NVP-LAQ824: from concept to clinic. Curr Med Chem 2003;10(22):2393–402.
[10] Ito Y. Oncogenic potential of the RUNX gene family: 'overview'. Oncogene 2004;23(24):4198–208.
[11] Otto F, Thornell AP, Crompton T, Denzel A, Gilmour KC, Rosewell IR, et al. Cbfa1, a candidate gene for cleidocranial dysplasia syndrome, is essential for osteoblast differentiation and bone development. Cell 1997;89:765–71.
[12] Li QL, Ito K, Sakakura C, Fukamachi H, Inoue K, Chi XZ, et al. Causal relationship between the loss of RUNX3 expression and gastric cancer. Cell 2002;109(1):113–24.
[13] Ito K, Liu Q, Salto-Tellez M, Yano T, Tada K, Ida H, et al. RUNX3, a novel tumor suppressor, is highly inactivated in gastric cancer by protein mislocalization. Cancer Res 2005;65:7743–50.
[14] Chi XZ, Yang JO, Lee KY, Ito K, Sakakura C, Li QL, et al. RUNX3 suppresses gastric epithelial cell growth by inducing p21(WAF1/Cip1) expression in cooperation with transforming growth factor {beta}-activated SMAD. Mol Cell Biol 2005;25(18):8097–107.
[16] Lau QC, Raja E, Salto-Tellez M, Liu Q, Ito K, Inoue M, et al. RUNX3 is frequently inactivated by dual mechanisms of protein mislocalization and promoter hypermethylation in breast cancer. Cancer Res 2006;66(13):6512–20.
[17] Imamura Y, Hibi K, Koike M, Fujiwara M, Kodera Y, Ito K, et al. RUNX3 promoter region is specifically methylated in poorly-differentiated colorectal cancer. Anticancer Res 2005;25(4):2627–30.
[18] Sato K, Tomizawa Y, Iijima H, Saito R, Ishizuka T, Nakajima T, et al. Epigenetic inactivation of the RUNX3 gene in lung cancer. Oncol Rep 2006;15(1):129–35.
[19] Park WS, Cho YG, Kim CJ, Song JH, Lee YS, Kim SY, et al. Hypermethylation of the RUNX3 gene in hepatocellular carcinoma. Exp Mol Med 2005;37(4):276–81.
[20] Kang GH, Lee S, Lee HJ, Hwang KS. Aberrant CpG island hypermethylation of multiple genes in prostate cancer and prostatic intraepithelial neoplasia. J Pathol 2004;202(2):233–40.
[21] Ruefli AA, Smyth SM, Johnstone RW. HMBA induces activation of a caspase-independent cell death pathway to overcome P-glycoprotein-mediated multidrug resistance. Blood 2000;95(7):2378–85.
[22] Van Lint C, Emiliani S, Verdin E. The expression of a small fraction of cellular genes is changed in response to histone hyperacetylation. Gen Express 1996;5:245–53.
[23] Richon VM, Zhou X, Rifkind RA, Marks PA. Histone deacetylase inhibitors: development of suberoylanilide hydroxamic acid (SAHA) for the treatment of cancers. Blood Cells Mol Dis 2001;27:260–4.
[24] Romanski A, Bacic B, Bug G, Preifer H, Gul H, Remiszewski S, et al. Use of a novel histone deacetylase inhibitor to induce apoptosis in cell lines of acute lymphoblastic leukemia. Haematologica 2004;89:419–26.
[25] Kagoshima H, Akamatsu Y, Ito Y, Shigesada K. Functional dissection of the α and β subunits of transcription factor PEBP2 and the Redox susceptibility of Its DNA binding activity. J Biol Chem 1996;20;271(51):33074–82.
[26] Rountree MR, Bachman KE, Herman JG, Baylin SB. DNA methylation, chromatin inheritance, and cancer. Oncogene 2001;20(24):3156–65.
[27] Bachman KE, Rountree MR, Baylin SB. Dnmt3a and Dnmt3b are transcriptional repressors that exhibit unique localization properties to heterochromatin. J Biol Chem 2001;276(34):32282–7.
[28] Robertson KD, Ait-Si-Ali S, Yokochi T, Wade PA, Jones PL, Wolffe AP. DNMT1 forms a complex with Rb, E2F1 and HDAC1 and represses transcription from E2F-responsive promoters. Nat Genet 2000;25:338–42.
[29] Cameron EE, Bachman KE, Myohanen S, Herman JG, Baylin SB. Synergy of demethylation and histone deacetylase inhibition in the re-expression of genes silenced in cancer. Nat Genet 1999;21(1):103–7.

[30] Primeau M, Gagnon J, Momparler RL. Synergistic antineoplastic action of DNA methylation inhibitor 5-AZA-2′-deoxycytidine and histone deacetylase inhibitor depsipeptide on human breast carcinoma cells. Int J Cancer 2003;103(2):177–84.
[31] Ito Y, Miyazono K. RUNX transcription factors as key targets of TGF-β superfamily signaling. Curr Opin Genet Dev 2003;13:43–7.
[32] Hannon GJ, Beach D. $p15^{INK4B}$ is a potential effector of TGF-beta-induced cell cycle arrest. Nature 1994;371:257–61.
[33] Reynisdottir I, Polyak K, Iavarone A, Massague J. Kip/Cip and Ink4 cdk inhibitors cooperate to induce cell cycle arrest in response to TGF-beta. Genes Dev 1995;9:1831–45.
[34] Koeller KM, Haggarty SJ, Perkins BD, Leykin L, Wong JC, Kao MC, et al. Chemical genetic modifier screens: small molecule trichostatin suppressors as probes of intracellular histone and tubulin acetylation. Chem Biol 2003;10(5):397–410.
[35] Kim JS, Lee S, Lee T, Trepel JB, Lee Y-W. Transcriptional activation of p21WAF1/CIP1 by Apicidin, a novel histone deacetylase inhibitor. Biochem Biophys Res Commun 2001;281:866–71.
[36] Peart MJ, Smyth GK, van Laar RK, Bowtell DD, Richon VM, Marks PA, et al. Identification and functional significance of genes regulated by structurally different histone deacetylase inhibitors. Proc Natl Acad Sci USA 2005;102(10):3697–702.
[37] Ruefli AA, Ausserlechner MJ, Bernhard D, Sutton VR, Tainton KM, Kofler R, et al. The histone deacetylase inhibitor and chemotherapeutic agent suberoylanilide hydroxamic acid (SAHA) induces a cell-death pathway characterized by cleavage of Bid and production of reactive oxygen species. Proc Natl Acad Sci USA 2001;98(19):10833–8.
[38] Henderson C, Mizzau M, Paroni G, Maestro R, Schneider C, Brancolini C. Role of caspases, Bid, and p53 in the apoptotic response triggered by histone deacetylase inhibitors trichostatin-A (TSA) and suberoylanilide hydroxamic acid (SAHA). J Biol Chem 2003;278(14):12579–8.
[39] Yano T, Ito K, Fukamachi H, Chi XZ, Wee HJ, Inoue K, et al. The RUNX3 tumor suppressor upregulates Bim in gastric epithelial cells undergoing transforming growth factor beta-induced apoptosis. Mol Cell Biol 2006;26(12):4474–88.
[40] Yamamura Y, Lee WL, Inoue K, Ida H, Ito Y. RUNX3 cooperates with FoxO3a to induce apoptosis in gastric cancer cells. J Biol Chem 2006;281(8):5267–76.
[41] Cohen LA, Amin S, Marks PA, Rifkind RA, Desai D, Richon VM. Chemoprevention of carcinogen-induced mammary tumorigenesis by the hybrid polar cytodifferentiation agent, suberanilohydroxamic acid (SAHA). Anticancer Res 1999;19(6B):4999–5005.